

MHC class I modulates NMDA receptor function and AMPA receptor trafficking

Lawrence Fourgeaud^{a,1}, Christopher M. Davenport^a, Carolyn M. Tyler^b, Timothy T. Cheng^a, Michael B. Spencer^a, and Lisa M. Boulanger^{a,c,2,3}

^aDivision of Biological Sciences, Section of Neurobiology, and ^cSilvio Varon Chair in Neuroregeneration, University of California at San Diego, La Jolla, CA 92093-0366; and ^bDepartment of Molecular Biology and Princeton Neuroscience Institute, Princeton University, Princeton, NJ 08544

Edited by Richard L. Huganir, The Johns Hopkins University School of Medicine, Baltimore, MD, and approved October 28, 2010 (received for review December 4, 2009)

Proteins of the major histocompatibility complex class I (MHCI) are known for their role in immunity and have recently been implicated in long-term plasticity of excitatory synaptic transmission. However, the mechanisms by which MHCI influences synaptic plasticity remain unknown. Here we show that endogenous MHCI regulates synaptic responses mediated by NMDA-type glutamate receptors (NMDARs) in the mammalian central nervous system (CNS). The AMPA/NMDA ratio is decreased at MHCI-deficient hippocampal synapses, reflecting an increase in NMDAR-mediated currents. This enhanced NMDAR response is not associated with changes in the levels, subunit composition, or gross subcellular distribution of NMDARs. Increased NMDAR-mediated currents in MHCI-deficient neurons are associated with characteristic changes in AMPA receptor trafficking in response to NMDAR activation. Thus, endogenous MHCI tonically inhibits NMDAR function and controls downstream NMDAR-induced AMPA receptor trafficking during the expression of plasticity.

immune | GluR | hippocampus

Proteins of the major histocompatibility complex class I (MHCI) are best known for their role in adaptive immunity, but several lines of evidence suggest they also have nonimmune functions in neurons (1, 2). MHCI is expressed by healthy neurons in the developing and adult CNS (3–7). Neuronal MHCI mRNA levels are dynamic during development and are regulated by electrical activity (3, 4) and by the cAMP-response element-binding protein (CREB) (8). MHCI protein is enriched in synaptic fractions (4) and is detected in hippocampal dendritic spines, where it colocalizes with PSD-95 (9).

Studies in mice genetically deficient for cell-surface MHCI ($\beta 2m^{-/-}TAP^{-/-}$ mice) suggest a role for MHCI in activity-dependent plasticity. In MHCI-deficient mice, NMDA receptor (NMDAR)-dependent hippocampal long-term potentiation (LTP) is enhanced, whereas long-term depression (LTD) is abolished (4). Although the mechanisms by which MHCI mediates immune signaling have been relatively well characterized, nothing is known about how MHCI contributes to NMDAR-dependent plasticity in vitro or in vivo.

In the adult hippocampus, plasticity induced by activation of NMDARs is expressed as changes in the trafficking and function of AMPA receptors (AMPA) (10–13). In current models, the magnitude and kinetics of NMDAR activation determine whether potentiation or depression is induced, with large, transient NMDAR activation causing LTP and smaller, longer-lasting activation causing LTD (14, 15). Therefore, to better understand the role of endogenous MHCI in the induction or expression of synaptic plasticity, we examined the levels, distribution, trafficking, and function of AMPA- and NMDA-type receptors in MHCI-deficient hippocampal neurons.

The current experiments reveal an unexpected role for postsynaptic MHCI in controlling NMDAR function. Loss of MHCI causes a drop in the AMPA/NMDA ratio and an enhancement of NMDAR-mediated responses at CA3–CA1 synapses. This enhancement cannot be attributed to changes in the levels, subunit composition, or gross subcellular distribution of NMDARs.

The increase in basal NMDAR-mediated responses in MHCI-deficient neurons is not associated with a change in basal AMPAR properties but is associated with changes in the trafficking of AMPARs in response to NMDA. Thus, in addition to its immune role, MHCI restricts NMDAR function and controls downstream NMDAR-induced AMPAR trafficking.

Results

Basal AMPAR- and NMDAR-Mediated Synaptic Responses. To test if MHCI affects the induction of plasticity by modifying basal glutamatergic transmission, whole-cell voltage-clamp recordings were performed at Schaffer collateral/CA1 synapses in acute hippocampal slices from WT or MHCI-deficient ($\beta 2m^{-/-}TAP^{-/-}$; *Materials and Methods*) animals. AMPAR-mediated responses decay rapidly after reaching their peak, whereas NMDAR-mediated responses decay over a longer time course. These differential decay kinetics were used to determine the proportion of the excitatory postsynaptic current (EPSC) mediated by AMPARs versus NMDARs (*Materials and Methods*). At $\beta 2m^{-/-}TAP^{-/-}$ synapses, the AMPA/NMDA ratio was significantly lower than at WT synapses (Fig. 1A; WT 2.0 ± 0.1 , $n = 15$ cells; $\beta 2m^{-/-}TAP^{-/-}$ 1.5 ± 0.1 , $n = 12$ cells; $*P < 0.05$, two-tailed unpaired t test). Similar results were obtained when NMDAR-mediated currents were isolated by pharmacologically blocking AMPARs (Fig. S1).

The lower AMPA/NMDA ratio in MHCI-deficient neurons could reflect an increase in the NMDAR-mediated response and/or a decrease in the AMPAR-mediated response. To distinguish among these possibilities, we performed extracellular recordings and plotted the input–output (I/O) relationship for pharmacologically isolated AMPAR- and NMDAR-mediated components of the field excitatory postsynaptic potential (fEPSP). The I/O relationships of the AMPAR and NMDAR components were linear across a range of stimulation intensities in both genotypes (Fig. 1B and C). Although the slope of the AMPAR I/O curve was comparable in WT and $\beta 2m^{-/-}TAP^{-/-}$ slices (Fig. 1B), the slope of the I/O curve for NMDAR-mediated responses was significantly steeper in $\beta 2m^{-/-}TAP^{-/-}$ slices (Fig. 1C; mean NMDAR-mediated I/O slopes: WT 0.21 ± 0.04 , $n = 6$ animals; $\beta 2m^{-/-}TAP^{-/-}$ 0.41 ± 0.08 , $n = 7$ animals; $P < 0.05$). This increase in the NMDAR I/O slope is sufficient to fully account for the drop in the AMPA/NMDA ratio in MHCI-deficient animals and suggests that loss

Author contributions: L.F. and L.M.B. designed research; L.F., C.M.D., and C.M.T. performed research; L.F., T.T.C., M.B.S., and L.M.B. analyzed data; and L.F. and L.M.B. wrote the paper.

The authors declare no conflict of interest.

This article is a PNAS Direct Submission.

¹Present address: Molecular Neurobiology Laboratory, Salk Institute for Biological Studies, La Jolla, CA 92037.

²Present address: Department of Molecular Biology and Princeton Neuroscience Institute, Princeton University, Princeton, NJ 08544.

³To whom correspondence should be addressed. E-mail: lboulang@princeton.edu.

This article contains supporting information online at www.pnas.org/lookup/suppl/doi:10.1073/pnas.0914064107/-DCSupplemental.

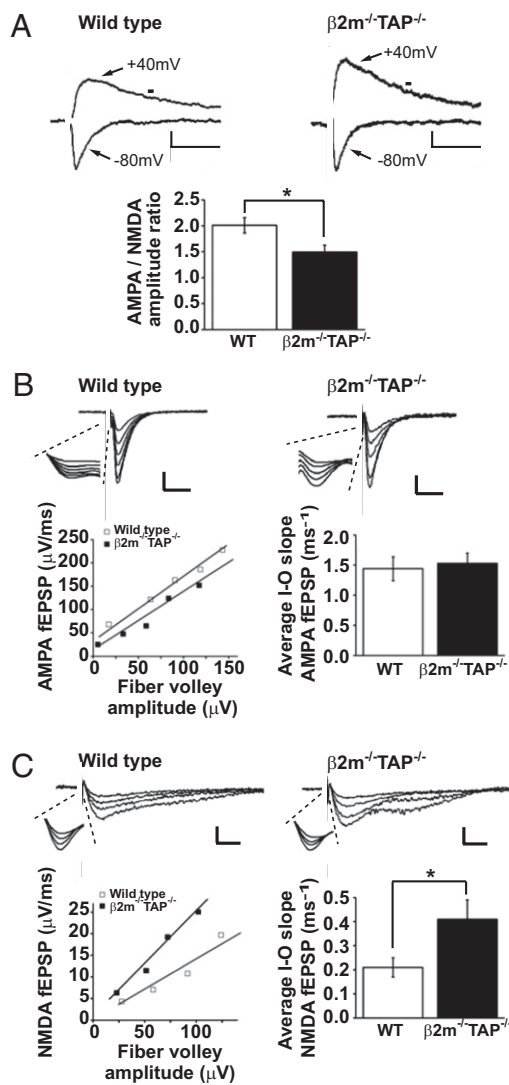


Fig. 1. Increased NMDAR-mediated responses in $\beta 2m^{-/-}TAP^{-/-}$ hippocampal slice. (A Upper) Representative EPSCs recorded from individual CA1 pyramidal neurons voltage-clamped at -80 mV or $+40$ mV. NMDAR-mediated currents were measured at the time marked with horizontal bar. (Scale bar: WT, 20 pA/50 ms; $\beta 2m^{-/-}TAP^{-/-}$, 10 pA/50 ms.) (Lower) Mean AMPA/NMDA ratio in CA1 neurons is significantly decreased in $\beta 2m^{-/-}TAP^{-/-}$ animals. (B Upper) Representative AMPAR-mediated fEPSPs recorded in D(-)-2-Amino-5-phosphopentanoic acid (D-APV) from CA1 dendrites in WT or $\beta 2m^{-/-}TAP^{-/-}$ hippocampal slices. (Scale bar: WT, 0.2 mV/20 ms; $\beta 2m^{-/-}TAP^{-/-}$, 0.1 mV/20 ms.) (Insets) Magnified view of the fiber volley. (Lower Left) I/O relationship of the AMPAR-mediated responses in the examples above. (Lower Right) Summary graph showing mean AMPAR-mediated I/O slopes (WT, $n = 8$ animals; $\beta 2m^{-/-}TAP^{-/-}$, $n = 8$ animals). (C Upper) Representative NMDAR-mediated fEPSPs recorded in 6,7-dinitroquinoxaline-2,3-dione (DNQX) from CA1 dendrites in WT or $\beta 2m^{-/-}TAP^{-/-}$ hippocampal slices. (Scale bar: 0.1 mV/20 ms.) (Insets) Magnified view of the fiber volley. (Lower Left) I/O relationship of the NMDAR-mediated responses in the examples above. (Lower Right) Summary graph showing mean NMDAR-mediated I/O slopes (for values, see text).

of MHCI causes a disinhibition of NMDAR-mediated synaptic responses.

Source of Increased NMDAR-Mediated Responses in $\beta 2m^{-/-}TAP^{-/-}$ Hippocampal Neurons. The enhanced NMDAR-mediated responses in $\beta 2m^{-/-}TAP^{-/-}$ neurons might reflect an increase in the proportion of NMDAR-containing, AMPAR-free (“silent”) synapses or an increase in the NMDAR-mediated response per

synapse. Although silent synapses do not contribute significantly to synaptic transmission at resting membrane potentials, because of blockade of the channel by Mg^{2+} , they could have been unsilenced in the above experiments (by depolarization to $+40$ mV in the AMPA/NMDA ratio recordings or by lowering extracellular Mg^{2+} in the I/O recordings). To estimate the fraction of silent synapses, we measured the coefficient of variation (CV) of EPSCs evoked by Schaffer collateral stimulation at different holding membrane potentials. The CV of the EPSCs drops when silent synapses are unsilenced and macroscopic currents are comprised of summed activity at a larger number of postsynaptic sites. When the holding potential was switched from -80 mV to $+40$ mV, the CV dropped to a comparable extent for both WT and $\beta 2m^{-/-}TAP^{-/-}$, suggesting that silent synapses are present in similar proportions regardless of the level of MHCI (Fig. 2A). Thus, it is unlikely that the increase in NMDAR-mediated responses in $\beta 2m^{-/-}TAP^{-/-}$ neurons is caused by an increase in the number of silent synapses. Rather, more of the glutamatergic synaptic transmission is mediated by NMDARs at $\beta 2m^{-/-}TAP^{-/-}$ synapses.

An increase in NMDAR-mediated responses could also be caused by changes in NMDAR subunit composition. Most NMDARs are heterotetramers consisting of two obligatory NR1

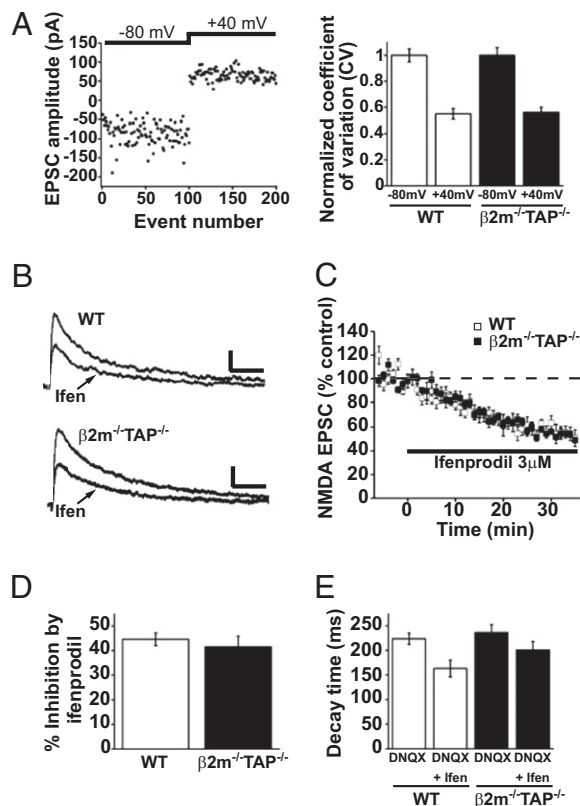


Fig. 2. Normal proportions of silent synapses and NR2B-containing NMDARs in $\beta 2m^{-/-}TAP^{-/-}$ hippocampal neurons. (A Left) Sample plot of EPSC amplitudes for individual consecutive events recorded from a WT CA1 neuron voltage-clamped at -80 mV and then shifted to $+40$ mV. (Right) Summary graph showing the mean CV of EPSCs at -80 mV and $+40$ mV, normalized to the CV at -80 mV (WT $n = 9$ cells; $\beta 2m^{-/-}TAP^{-/-}$ $n = 8$ cells). (B) Representative NMDAR-mediated EPSCs recorded from individual WT (Upper) or $\beta 2m^{-/-}TAP^{-/-}$ (Lower) CA1 neurons 6 min before or 30 min after application of ifenprodil. (Scale bar: 20 pA/100 ms.) (C) Averaged NMDAR-mediated EPSCs recorded before and during bath application of $3 \mu M$ ifenprodil, normalized to a 6-min baseline (WT $n = 7$ cells; $\beta 2m^{-/-}TAP^{-/-}$ $n = 8$ cells). (D) Mean percentage inhibition of the normalized NMDAR-mediated EPSC amplitude by ifenprodil. (E) Mean decay time of the NMDAR-mediated EPSC measured 6 min before or 30 min after application of ifenprodil.

subunits paired with two NR2 subunits (NR2A–NR2D). NR2A-containing NMDARs have relatively rapid decay kinetics, whereas NR2B-containing NMDARs, which are more common early in development, have relatively slow decay kinetics (16, 17). An increase in the proportion of NR2B-containing NMDARs can prolong NMDAR activation, enhancing temporal integration and increasing the amplitude of the whole-cell NMDAR-mediated current (18). However, the basal decay kinetics of NMDAR-mediated currents are unchanged in MHCI-deficient neurons (Fig. 2E), suggesting that the proportion of NR2B-containing NMDARs may not be altered. To directly determine the contribution of NR2B-containing NMDARs, the component of the EPSC mediated by NR2B-containing NMDARs was blocked with ifenprodil (19, 20). As expected, bath application of ifenprodil caused a reduction of the amplitude and acceleration of the decay of NMDAR-mediated currents that stabilized within 30 min (Fig. 2B–E). Ifenprodil blocked a similar proportion of the NMDAR currents in both genotypes, indicating that NR2B-containing NMDARs make up a normal percentage of the synaptic pool of NMDARs in $\beta 2m^{-/-}TAP^{-/-}$ synapses (Fig. 2D). Furthermore, endogenous cell-surface NR2B-containing NMDARs were immunolabeled in cultured hippocampal neurons. The intensity of NR2B labeling on the surface of dendrites was indistinguishable in WT and $\beta 2m^{-/-}TAP^{-/-}$ neurons (Fig. S2B). Thus, three independent measures (EPSC decay kinetics, ifenprodil sensitivity, and NR2B immunostaining) indicate that MHCI does not affect the proportion of NMDAR-mediated currents carried by NR2B-containing receptors. Rather, these results are consistent with the idea that MHCI limits the current carried by both NR2B- and non-NR2B-containing receptors.

Higher levels of the obligatory subunit NR1 at $\beta 2m^{-/-}TAP^{-/-}$ synapses could increase the synaptic NMDAR current without affecting the relative contributions of different NR2 subunits. Synaptic levels of NR1 were first evaluated by examining the extent of the colocalization between endogenous NR1 and known synaptic markers in hippocampal neurons in culture. As expected, in mature WT neurons, punctiform NR1 labeling colocalized with PSD-95, a marker of the postsynaptic density, and was directly apposed to SV2, a marker of the presynaptic terminal (Fig. 3A and B). In $\beta 2m^{-/-}TAP^{-/-}$ neurons, the intensity and degree of colocalization of NR1 with PSD-95 and SV2 was qualitatively similar to levels found for WT neurons (Fig. 3A and B). Quantitative analysis confirmed that the average degree of colocalization between NR1 and PSD-95 or SV2 was similar in WT and MHCI-deficient neurons (Fig. 3C). To further examine NR1 expression, we performed subcellular fractionation experiments on microdissected hippocampi and compared NR1 levels in Western blots of total (S1) and synaptic (P3) fractions between WT and $\beta 2m^{-/-}TAP^{-/-}$ animals. Synaptic fractions were enriched for the synaptically localized protein synaptophysin, demonstrating effective extraction and enrichment of synaptic proteins (Fig. 3D). Both total and synaptic levels of NR1 were indistinguishable between WT and $\beta 2m^{-/-}TAP^{-/-}$ hippocampal lysates (Fig. 3D and E). Additional biochemical experiments showed that the levels of NR1 are also indistinguishable in synaptosomal and PSD fractions from WT versus MHCI-deficient neurons ($\beta 2m^{-/-}TAP^{-/-}$ NR1 levels, normalized to WT: synaptosomal fraction, 1.08; PSD fraction, 0.96; $n = 2$). Finally, endogenous cell-surface NR1 was immunolabeled in cultured hippocampal neurons. Characteristic, punctuate NR1 staining was observed on the surface of dendrites in WT and $\beta 2m^{-/-}TAP^{-/-}$ neurons. Quantitative analysis showed no increase but a modest yet significant decrease in the intensity of NR1 labeling in proximal dendrites in $\beta 2m^{-/-}TAP^{-/-}$ neurons (Fig. S2). Because NR1 is an obligatory subunit of all NMDARs, the relative stability of NR1 levels and localization in both immunocytochemical and biochemical assays is not consistent with an increase in the number of functional NMDARs in $\beta 2m^{-/-}TAP^{-/-}$ hippocampal neurons.

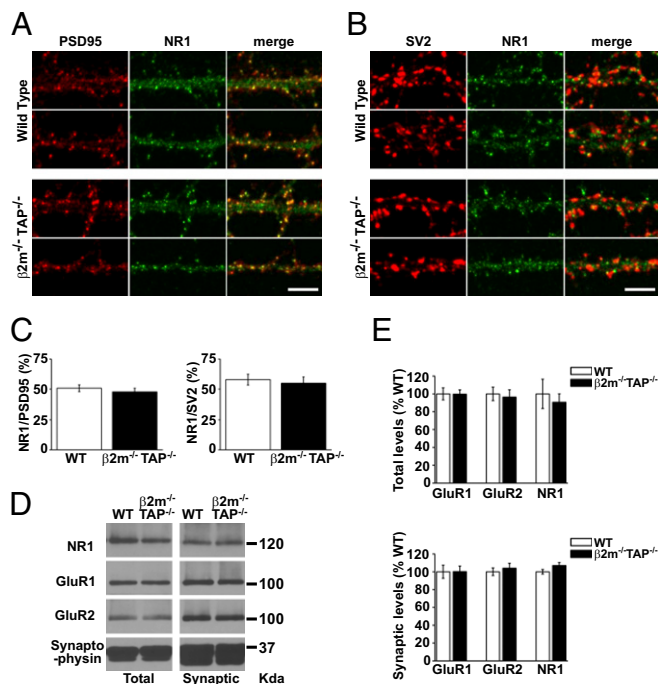


Fig. 3. Total and synaptic levels of NR1, GluR1, and GluR2 are not increased in $\beta 2m^{-/-}TAP^{-/-}$ hippocampal neurons. (A) Representative NR1 and PSD-95 double-label immunostaining in straightened proximal dendrites from WT and $\beta 2m^{-/-}TAP^{-/-}$ hippocampal neurons in culture. (Scale bar: 5 μ m.) (B) Representative NR1 and SV2 double-label immunostaining in straightened proximal dendrites from WT and $\beta 2m^{-/-}TAP^{-/-}$ hippocampal neurons in culture. (Scale bar: 5 μ m.) (C) Mean percentage of NR1 puncta colocalizing with PSD-95 puncta (Left; WT $n = 12$ cells; $\beta 2m^{-/-}TAP^{-/-} n = 13$ cells) or SV2 puncta (Right; WT $n = 11$ cells; $\beta 2m^{-/-}TAP^{-/-} n = 12$ cells) in WT versus $\beta 2m^{-/-}TAP^{-/-}$ hippocampal neurons in culture (two separate experiments). Colocalization was defined as contact between puncta at the light level, and therefore includes closely apposed as well as extensively overlapping puncta. (D) Representative Western blot of total (S1) and synaptic plasma membrane-enriched (P3) fractions from WT and $\beta 2m^{-/-}TAP^{-/-}$ mouse hippocampi probed for NR1, GluR1, GluR2, and synaptophysin. (E) Total (Upper) or synaptic (Lower) levels of GluR1, GluR2, and NR1 in samples from four WT and four $\beta 2m^{-/-}TAP^{-/-}$ animals, normalized to synaptophysin and represented as percentage of WT.

Changes in the synaptic contribution of NR3 subunits (21) could also potentially account for the increase in NMDAR-mediated current observed in $\beta 2m^{-/-}TAP^{-/-}$ neurons. However, total and synaptic levels of NR3A were similar between WT and $\beta 2m^{-/-}TAP^{-/-}$ hippocampal lysates (Fig. S3). Together, our results suggest that MHCI limits the function of NMDARs without affecting receptor levels, subunit composition, or gross subcellular localization.

NMDA-Induced Changes in AMPAR Trafficking. Activation of NMDARs gives rise to characteristic patterns of AMPAR trafficking during the expression of NMDAR-dependent plasticity. For example, brief bath application of NMDA causes a long-lasting NMDAR-dependent synaptic depression in WT hippocampus that is associated with removal of AMPARs from the cell surface (22–24). Therefore, to assess the impact of MHCI on NMDAR-induced AMPAR trafficking, we measured cell-surface levels of the AMPAR subunits GluR1 and GluR2 before and after direct stimulation of NMDARs. Subcellular fractionation experiments showed that basal total and synaptic levels of GluR1 and GluR2 were indistinguishable from WT in $\beta 2m^{-/-}TAP^{-/-}$ hippocampal lysates (Fig. 3D and E). Similarly, characteristic, punctuate cell-surface GluR1 and GluR2 labeling was observed on dendrites of both WT and $\beta 2m^{-/-}TAP^{-/-}$ cultured hippocampal neurons before NMDA treatment (Fig. 4A and C), and

A second possibility is that MHCI affects the population of NMDARs that are localized to synaptic versus immediately perisynaptic compartments. Synaptic levels of NR1 are not altered in biochemical fractionation experiments, but this method enriches synaptic as well as immediately perisynaptic receptors, the latter of which are not thought to contribute to basal synaptic transmission. Thus, a reallocation of NMDARs from perisynaptic to synaptic sites in $\beta 2m^{-/-}TAP^{-/-}$ neurons could yield an increase in NMDAR-mediated responses without an apparent change in NMDAR synaptic levels, when measured biochemically. However, more spatially precise immunostaining experiments show that the colocalization of NR1 with markers of synaptic sites (SV2 and PSD-95) is unchanged in $\beta 2m^{-/-}TAP^{-/-}$ neurons, suggesting it is unlikely that changes in NR1 localization contribute significantly to the changes in NMDAR-mediated responses. In the future, immunoelectron microscopy could be used to determine whether MHCI affects the perisynaptic levels of NMDARs.

A third possibility is that MHCI mediates posttranslational changes in the functional properties of synaptic NMDARs. NMDARs are regulated posttranslationally by phosphorylation as well as by interactions with soluble cofactors [e.g., glycine, D-serine, Mg^{2+} , protons, zinc, polyamines, and dynorphin (17)] and transmembrane proteins [e.g., dopamine receptors, EphB receptors, and metabotropic glutamate receptors (31–33)]. Regardless of whether MHCI limits NMDARs directly or indirectly, the relevant modification may lie in the obligatory NR1 subunit because MHCI has similar effects on both NR2B- and non-NR2B-containing NMDARs.

MHCI is expressed in dendrites of hippocampal neurons, where it colocalizes with the postsynaptic marker PSD-95 (9), suggesting that MHCI could regulate dendritic NMDAR-mediated responses in a cell-autonomous manner (i.e., *in cis*). However, a recent study using immunogold electron microscopy found that MHCI is detectable at both pre- and postsynaptic sites in rat visual cortex (34). Until similar studies are conducted in the hippocampus, we cannot exclude the possibility that MHCI may also be expressed in presynaptic terminals in the hippocampus and may affect NMDAR-mediated responses *in trans*. Moreover, there is increasing evidence supporting a role for glial cells in modulating synaptic transmission, and NMDAR-mediated currents in particular (35, 36). In addition to being expressed by neurons, low levels of MHCI molecules are present on astrocytes and microglia in healthy brains (37, 38). Therefore, it is possible that MHCI regulates NMDARs through neuron–glia interactions.

A number of immunoreceptors that can bind to MHCI are expressed in the hippocampus, including PirB, Ly49, and KIR-like receptors (39–41). It is unlikely that MHCI affects NMDAR-dependent synaptic transmission via PirB, however, because recent studies show that LTP and LTD are normal in PirB knockouts (42). Further studies will be necessary to evaluate the role played by other immunoreceptors in MHCI functions at hippocampal synapses. Outside the CNS, MHCI is known to bind to cell-surface proteins both *in cis* and *in trans* (43). Studies consistent with a *trans* effect of MHCI on presynaptic ultrastructure and synapsin expression, as well as a *cis* effect on the scaling of the size of PSD-95 puncta in response to activity blockade, have recently been published (9). Thus, MHCI may have neuronal effects both *in cis* and *in trans*, depending on the brain region and function. Our current results suggest that the dominant changes in both basal synaptic transmission and plasticity in MHCI-deficient CA3–CA1 synapses occur postsynaptically. Thus, the most parsimonious explanation is that postsynaptically expressed MHCI affects postsynaptic NMDAR-mediated responses in a cell-autonomous manner. Similar modulation of NMDAR function *in cis* has been demonstrated for other transmembrane proteins, including dopamine receptors and EphB receptors (31, 33).

Given the central importance of NMDARs in the control of gene expression, brain development, synaptic plasticity, learning and memory, and excitotoxicity as well as accumulating evidence

of glutamatergic dysfunction in neurological disorders, including autism and schizophrenia (28), it is essential to understand mechanisms that control NMDAR efficacy. Here we provide evidence that endogenous MHCI limits NMDAR currents in the mammalian CNS. MHCI levels are dynamic during development and are regulated by activity (3), and thus our results suggest a mechanism whereby changes in MHCI levels could link developmental stage and synaptic activity to physiological changes in the rules governing synaptic plasticity *in vivo*. Neuronal MHCI levels are also increased during inflammation (44), seizures (3), injury (45), and aging (46). By limiting NMDAR function, higher levels of MHCI under these conditions could prevent runaway potentiation and act as an endogenous neuroprotective against NMDAR-mediated excitotoxicity.

Materials and Methods

Mice. Experiments were performed on commercially available C57BL/6 mice and MHCI-deficient mice in a C57BL/6 background, backcrossed more than nine times to WT. Because many MHCI genes are expressed in neurons, we made use of mice genetically deficient for two molecules required for the stable cell-surface expression of nearly all MHCI proteins: $\beta 2$ -microglobulin ($\beta 2m$), an obligatory MHCI subunit, and the transporter associated with antigen processing (TAP1), a transporter required to load peptides onto mature MHCI proteins (47–49). Animals lacking these two proteins ($\beta 2m^{-/-}TAP^{-/-}$ double mutants) are immune-compromised but are outwardly normal when kept in a clean facility. All mice were age- and sex-matched within experiments, and procedures were performed according to institutional guidelines and protocols approved by the University of California at San Diego Institutional Animal Care and Use Committee.

Electrophysiology. Acute coronal brain slices (350 μm) were prepared from postnatal day 13 (P13) to P16 C57BL/6 WT or $\beta 2m^{-/-}TAP^{-/-}$ mice. Visualized whole-cell patch-clamp recordings of evoked EPSCs from individual CA1 pyramidal neurons and field recordings from populations of CA1 pyramidal cells were conducted at room temperature ($\sim 25^{\circ}C$) with standard methods. See *SI Materials and Methods* for details.

Hippocampal Cultures. Low-density cultures of acutely dissociated hippocampal neurons were prepared from newborn (P0) WT and $\beta 2m^{-/-}TAP^{-/-}$ mice by using a protocol adapted from ref. 50. See *SI Materials and Methods* for details.

Glutamate Receptor Immunocytochemistry. Surface labeling. Endogenous AMPARs and NMDARs were labeled in hippocampal neurons in culture with antibodies directed against the extracellular domain of GluR1 (rabbit anti-GluR1; Calbiochem), GluR2 (mouse anti-GluR2 clone 6C4; Zymed), NR1 (mouse anti-NR1 clone 54.1; BD Pharmingen), or NR2B (mouse anti-NR2B clone N59/20; NeuroMab).

Double-label immunostaining. Hippocampal neurons were double-labeled with anti-NR1 (rabbit anti-NR1; Millipore) and anti-PSD-95 (mouse anti-PSD-95 clone K28/43; NeuroMab) or anti-SV2 (mouse anti-SV2 clone SP2/0; Developmental Studies Hybridoma Bank). See *SI Materials and Methods* for details.

Image Acquisition and Quantification. Surface labeling. Images were acquired by using an epifluorescence microscope (Olympus BX51WI) equipped with a CCD camera (Qimaging Retiga 2000R). For comparisons between genotypes, all images were acquired the same day using identical acquisition settings. Images were quantified by an observer blind to genotype with ImageJ software (National Institutes of Health, version 1.37). See *SI Materials and Methods* for details.

Double-label immunostaining. Images were acquired by using an inverted microscope (Leica DMI6000) outfitted with a spinning disk confocal head (Yokogawa) and equipped with a cooled CCD camera (Hamamatsu). For comparisons between genotypes, all images were acquired the same day using identical acquisition settings. Maximum projected confocal Z-stacks are displayed.

Subcellular Fractionation. For each experiment, two 4- to 5-wk-old animals of each genotype were used. Subcellular fractionation was performed as previously described (51). See *SI Materials and Methods* for details.

Western Blot Analysis. Protein quantification was performed by using a BCA protein assay kit (Pierce) according to the manufacturer's instructions. Thirty

micrograms of each sample was subjected to SDS/PAGE, transferred to a PVDF membrane, and probed with antibodies directed against proteins of interest: GluR1 (rabbit anti-GluR1, 0.1 $\mu\text{g}/\text{mL}$; Chemicon), GluR2 (mouse anti-GluR2 clone 6C4, 0.5 $\mu\text{g}/\text{mL}$; Zymed), NR1 (mouse anti-NR1 clone 54.1, 0.5 $\mu\text{g}/\text{mL}$; BD Pharmingen), NR3A (rabbit anti-NR3A, 1 $\mu\text{g}/\text{mL}$; Chemicon), and synaptophysin (clone SY38, 0.3 $\mu\text{g}/\text{mL}$; Chemicon). Relative band intensity was quantified by densitometric analysis with ImageJ software (National Institutes of Health, version 1.37). Sample bands were normalized to synaptophysin and averaged across experiments.

Statistics. For all experiments, means are reported \pm SEM. Statistical comparisons of the data were performed with GraphPad InStat version 3.06 for Windows (GraphPad Software).

ACKNOWLEDGMENTS. We thank M. Chacon for synaptosomal and PSD fractionation; J. Bosze and D. Lee for technical assistance; M. Scanziani,

J. Isaacson, A. Ghosh, M. McDonald, and T. Dixon-Salazar for critical reading of the manuscript; D. Raullet (University of California, Berkeley, CA) and C. J. Shatz (Stanford University, Stanford, CA) for generously providing $\beta 2m^{-/-}TAP^{-/-}$ mice; and G. Lemke for his support. NR2B and PSD-95 antibodies were developed by and obtained from the University of California, Davis/ National Institute of Neurological Disorders and Stroke/National Institute of Mental Health NeuroMab Facility (National Institutes of Health Grant U24NS050606). SV2 monoclonal antibody was developed by Kathleen M. Buckley, obtained from the Developmental Studies Hybridoma Bank, developed under the auspices of the National Institute of Child Health and Human Development, and maintained by the University of Iowa. Preliminary studies were supported by National Institute of Mental Health Grant MH 071666 (to C. J. Shatz). Experiments reported in this article were supported by a Sloan Research Fellowship and grants from the Whitehall Foundation, the Cure Autism Now Foundation (to L.M.B.), and Autism Speaks (to L.M.B. and L.F.).

- Boulanger LM, Shatz CJ (2004) Immune signalling in neural development, synaptic plasticity and disease. *Nat Rev Neurosci* 5:521–531.
- Fourgeaud L, Boulanger LM (2010) Role of immune molecules in the establishment and plasticity of glutamatergic synapses. *Eur J Neurosci* 32:207–217.
- Corriveau RA, Huh GS, Shatz CJ (1998) Regulation of class I MHC gene expression in the developing and mature CNS by neural activity. *Neuron* 21:505–520.
- Huh GS, et al. (2000) Functional requirement for class I MHC in CNS development and plasticity. *Science* 290:2155–2159.
- Lidman O, Olsson T, Piehl F (1999) Expression of nonclassical MHC class I (RT1-U) in certain neuronal populations of the central nervous system. *Eur J Neurosci* 11:4468–4472.
- Lindá H, Hammarberg H, Piehl F, Khademi M, Olsson T (1999) Expression of MHC class I heavy chain and $\beta 2$ -microglobulin in rat brainstem motoneurons and nigral dopaminergic neurons. *J Neuroimmunol* 101:76–86.
- Loconto J, et al. (2003) Functional expression of murine V2R pheromone receptors involves selective association with the M10 and M1 families of MHC class Ib molecules. *Cell* 112:607–618.
- Barco A, et al. (2005) Gene expression profiling of facilitated L-LTP in VP16-CREB mice reveals that BDNF is critical for the maintenance of LTP and its synaptic capture. *Neuron* 48:123–137.
- Goddard CA, Butts DA, Shatz CJ (2007) Regulation of CNS synapses by neuronal MHC class I. *Proc Natl Acad Sci USA* 104:6828–6833.
- Citri A, Malenka RC (2008) Synaptic plasticity: Multiple forms, and functions, and mechanisms. *Neurosciopharmacology* 33:18–41.
- Derkach VA, Oh MC, Guire ES, Soderling TR (2007) Regulatory mechanisms of AMPA receptors in synaptic plasticity. *Nat Rev Neurosci* 8:101–113.
- Kennedy MJ, Ehlers MD (2006) Organelles and trafficking machinery for postsynaptic plasticity. *Annu Rev Neurosci* 29:325–362.
- Shepherd JD, Huganir RL (2007) The cell biology of synaptic plasticity: AMPA receptor trafficking. *Annu Rev Cell Dev Biol* 23:613–643.
- Bliss TV, Collingridge GL (1993) A synaptic model of memory: Long-term potentiation in the hippocampus. *Nature* 361:31–39.
- Malenka RC, Bear MF (2004) LTP and LTD: An embarrassment of riches. *Neuron* 44:5–21.
- Paoletti P, Neyton J (2007) NMDA receptor subunits: Function and pharmacology. *Curr Opin Pharmacol* 7:39–47.
- Cull-Candy SG, Leszkiewicz DN (2004) Role of distinct NMDA receptor subtypes at central synapses. *Sci STKE* 2004:re16.
- Flint AC, Maisch US, Weishaupt JH, Kriegstein AR, Monyer H (1997) NR2A subunit expression shortens NMDA receptor synaptic currents in developing neocortex. *J Neurosci* 17:2469–2476.
- Tovar KR, Westbrook GL (1999) The incorporation of NMDA receptors with a distinct subunit composition at nascent hippocampal synapses in vitro. *J Neurosci* 19:4180–4188.
- Williams K (1993) Ifenprodil discriminates subtypes of the *N*-methyl-D-aspartate receptor: Selectivity and mechanisms at recombinant heteromeric receptors. *Mol Pharmacol* 44:851–859.
- Cavara NA, Hollmann M (2008) Shuffling the deck anew: How NR3 tweaks NMDA receptor function. *Mol Neurobiol* 38:16–26.
- Lee HK, Kameyama K, Huganir RL, Bear MF (1998) NMDA induces long-term synaptic depression and dephosphorylation of the GluR1 subunit of AMPA receptors in hippocampus. *Neuron* 21:1151–1162.
- Ehlers MD (2000) Reinsertion or degradation of AMPA receptors determined by activity-dependent endocytic sorting. *Neuron* 28:511–525.
- Lee SH, Simonetta A, Sheng M (2004) Subunit rules governing the sorting of internalized AMPA receptors in hippocampal neurons. *Neuron* 43:221–236.
- Holman D, Henley JM (2007) A novel method for monitoring the cell surface expression of heteromeric protein complexes in dispersed neurons and acute hippocampal slices. *J Neurosci Methods* 160:302–308.
- Park M, Penick EC, Edwards JG, Kauer JA, Ehlers MD (2004) Recycling endosomes supply AMPA receptors for LTP. *Science* 305:1972–1975.
- Lu W, et al. (2001) Activation of synaptic NMDA receptors induces membrane insertion of new AMPA receptors and LTP in cultured hippocampal neurons. *Neuron* 29:243–254.
- Lau CG, Zukin RS (2007) NMDA receptor trafficking in synaptic plasticity and neuropsychiatric disorders. *Nat Rev Neurosci* 8:413–426.
- Misra C, Brickley SG, Wyllie DJ, Cull-Candy SG (2000) Slow deactivation kinetics of NMDA receptors containing NR1 and NR2D subunits in rat cerebellar Purkinje cells. *J Physiol* 525:299–305.
- Perkel DJ, Nicoll RA (1993) Evidence for all-or-none regulation of neurotransmitter release: Implications for long-term potentiation. *J Physiol* 471:481–500.
- Lee FJ, et al. (2002) Dual regulation of NMDA receptor functions by direct protein-protein interactions with the dopamine D1 receptor. *Cell* 111:219–230.
- Perroy J, et al. (2008) Direct interaction enables cross-talk between ionotropic and group I metabotropic glutamate receptors. *J Biol Chem* 283:6799–6805.
- Takasu MA, Dalva MB, Zigmond RE, Greenberg ME (2002) Modulation of NMDA receptor-dependent calcium influx and gene expression through EphB receptors. *Science* 295:491–495.
- Needleman LA, Liu XB, El-Sabeawy F, Jones EG, McAllister AKMHC class I molecules are present both pre- and postsynaptically in the visual cortex during postnatal development and in adulthood. *Proc Natl Acad Sci USA* 107:16999–17004.
- Halassa MM, Haydon PG (2010) Integrated brain circuits: Astrocytic networks modulate neuronal activity and behavior. *Annu Rev Physiol* 72:335–355.
- Perea G, Navarrete M, Araque A (2009) Tripartite synapses: Astrocytes process and control synaptic information. *Trends Neurosci* 32:421–431.
- Steel CD, Hahto SM, Ciavarrá RP (2009) Peripheral dendritic cells are essential for both the innate and adaptive antiviral immune responses in the central nervous system. *Virology* 387:117–126.
- Wong GH, Bartlett PF, Clark-Lewis I, Battye F, Schrader JW (1984) Inducible expression of H-2 and Ia antigens on brain cells. *Nature* 310:688–691.
- Bryceson YT, Foster JA, Kuppusamy SP, Herkenham M, Long EO (2005) Expression of a killer cell receptor-like gene in plastic regions of the central nervous system. *J Neuroimmunol* 161:177–182.
- Syken J, Grandpre T, Kanold PO, Shatz CJ (2006) PirB restricts ocular-dominance plasticity in visual cortex. *Science* 313:1795–1800.
- Zohar O, et al. (2008) Cutting edge: MHC class I-Ly49 interaction regulates neuronal function. *J Immunol* 180:6447–6451.
- Raiker SJ, et al. (2010) Oligodendrocyte-myelin glycoprotein and Nogo negatively regulate activity-dependent synaptic plasticity. *J Neurosci* 30:12432–12445.
- Held W, Mariuzza RA (2008) Cis interactions of immunoreceptors with MHC and non-MHC ligands. *Nat Rev Immunol* 8:269–278.
- Foster JA, Quan N, Stern EL, Kristensson K, Herkenham M (2002) Induced neuronal expression of class I major histocompatibility complex mRNA in acute and chronic inflammation models. *J Neuroimmunol* 131:83–91.
- Thams S, Oliveira A, Cullheim S (2008) MHC class I expression and synaptic plasticity after nerve lesion. *Brain Res Brain Res Rev* 57:265–269.
- Edström E, Kullberg S, Ming Y, Zheng H, Ulfhake B (2004) MHC class I, $\beta 2$ microglobulin, and the INF- γ receptor are upregulated in aged motoneurons. *J Neurosci Res* 78:892–900.
- Ljunggren HG, et al. (1995) MHC class I expression and CD8+ T cell development in TAP1/ $\beta 2$ -microglobulin double mutant mice. *Int Immunol* 7:975–984.
- Van Kaer L, Ashton-Rickardt PG, Ploegh HL, Tonegawa S (1992) TAP1 mutant mice are deficient in antigen presentation, surface class I molecules, and CD4-8+ T cells. *Cell* 71:1205–1214.
- Zijlstra M, Li E, Sajjadi F, Subramani S, Jaenisch R (1989) Germ-line transmission of a disrupted $\beta 2$ -microglobulin gene produced by homologous recombination in embryonic stem cells. *Nature* 342:435–438.
- Banker G, Goslin K (1998) *Culturing Nerve Cells* (MIT Press, Cambridge, MA), 2nd Ed.
- Blackstone CD, et al. (1992) Biochemical characterization and localization of a non-N-methyl-D-aspartate glutamate receptor in rat brain. *J Neurochem* 58:1118–1126.